ORIGINAL ARTICLE

WILEY　Cancer Science

Periostin antisense oligonucleotide suppresses bleomycin-induced formation of a lung premetastatic niche for melanoma

Takashi Semba[1,2]　|　Eiji Sugihara[1,3] (iD)　|　Nagisa Kamoshita[1]　|　Sayaka Ueno[1]　|
Keitaro Fukuda[4]　|　Masafumi Yoshino[5]　|　Kazumasa Takao[5]　|　Kazunori Yoshikawa[5]　|
Kenji Izuhara[6]　|　Yoshimi Arima[1]　|　Makoto Suzuki[2]　|　Hideyuki Saya[1]

[1]Division of Gene Regulation, Institute for Advanced Medical Research, Keio University School of Medicine, Tokyo, Japan

[2]Department of Thoracic Surgery, Kumamoto University, Kumamoto, Japan

[3]Innovation Medical Research Institute, University of Tsukuba, Ibaraki, Japan

[4]Department of Dermatology, University of Massachusetts Medical School, Worcester, MA, USA

[5]AQUA Therapeutics Co., Ltd, Kobe, Japan

[6]Division of Medical Biochemistry, Department of Biomolecular Sciences, Saga Medical School, Saga, Japan

Correspondence
Eiji Sugihara, Division of Gene Regulation, Institute for Advanced Medical Research, Keio University School of Medicine, Tokyo, Japan.
Email: eiji77@z2.keio.jp

Metastasis is the leading cause of cancer death. A tumor-supportive microenvironment, or premetastatic niche, at potential secondary tumor sites plays an important role in metastasis, especially in tumor cell colonization. Although a fibrotic milieu is known to promote tumorigenesis and metastasis, the underlying molecular contributors to this effect have remained unclear. Here we show that periostin, a component of the extracellular matrix that functions in tissue remodeling, has a key role in formation of a fibrotic environment that promotes tumor metastatic colonization. We found that periostin was widely expressed in fibrotic lesions of mice with bleomycin-induced lung fibrosis, and that up-regulation of periostin expression coincided with activation of myofibroblasts positive for α-smooth muscle actin. We established a lung metastasis model for B16 murine melanoma cells and showed that metastatic colonization of the lung by these cells was markedly promoted by bleomycin-induced lung fibrosis. Inhibition of periostin expression by giving an intratracheal antisense oligonucleotide targeting periostin mRNA was found to suppress bleomycin-induced lung fibrosis and thereby to attenuate metastatic colonization of the lung by melanoma cells. Our results indicate that periostin is a key player in the development of bleomycin-induced fibrosis and consequent enhancement of tumor cell colonization in the lung. Our results therefore implicate periostin as a potential target for prevention or treatment of lung metastasis.

KEYWORDS
antisense oligonucleotide, lung fibrosis, melanoma, periostin, premetastatic niche

1 | INTRODUCTION

Lung metastasis is a major contributor to poor prognosis in many types of cancer, but the mechanisms of such metastasis remain largely unclear.[1,2] The formation of a tumor-supportive microenvironment, or premetastatic niche, by stromal components and immune cells is required for the colonization and propagation of circulating tumor cells at secondary or distant organs.[3] Remodeling of the extracellular matrix (ECM) is key to premetastatic niche formation and is induced by various events such as inflammation and tissue injury.[4] Fibrosis is a result of ECM remodeling. Preclinical data suggest that a fibrotic milieu promotes tumor cell colonization,[5,6]

Semba and Sugihara contributed equally to this work.

and smoking, one of the risk factors for pulmonary fibrosis, has been indicated to have an association with lung metastasis in breast cancer patients,[7] although the underlying molecular mechanism of this effect is unknown.

Periostin is a secreted ECM protein that plays various roles in tissue development and regeneration as well as contributing to conditions and diseases such as inflammation, allergy, fibrosis, and cancer.[8] A high level of periostin expression is associated with various types of cancer, including lung, breast, colorectal, and pancreatic cancer as well as melanoma.[9] Periostin is also implicated in lung metastasis of breast cancer as an important component of a cancer stem cell-supportive niche,[10] and it activates α-smooth muscle actin (α-SMA)-positive myofibroblasts and thereby promotes formation of a fibrotic microenvironment to sustain the metastatic growth of pancreatic cancer.[6] We previously reported that high mRNA expression of *POSTN*, *FN1*, and *COL1A1* was detected in the metastatic region of a melanoma patient by gene expression analysis, and that periostin was highly expressed during the wound-healing process.[11] Periostin was considered to be the most feasible therapeutic target among these ECM proteins because mice deficient in *Fn1* or *Col1a1* are embryonic lethal[12,13] whereas mice deficient in *Postn* develop normally. Thus, we showed that inhibition of periostin significantly reduced the incidence of melanoma metastasis to wound sites.[11] Although periostin is known to be an essential factor for fibrotic responses in idiopathic interstitial pneumonia in both mice and humans,[14,15] the relation between its role in lung fibrosis and lung metastasis of tumor cells is not well defined.

We have now established mice with pulmonary fibrosis induced by bleomycin as a lung metastasis model for melanoma. We found that fibrosis enhanced metastatic colonization of the lung of these animals by B16 murine melanoma cells, and that periostin contributed to formation of this premetastatic niche through activation of α-SMA[+] myofibroblasts. Furthermore, giving an intratracheal antisense oligonucleotide that targets periostin mRNA attenuated periostin expression as well as suppressed bleomycin-induced lung fibrosis and metastatic colonization of the lung by melanoma cells.

2 | MATERIALS AND METHODS

2.1 | Mice

Female C57BL/6J mice aged 6-10 weeks (Sankyo Labo Service Corporation, Tokyo, Japan) were studied. All animal experiments were carried out in accordance with protocols approved by the Ethics Committee of Keio University.

2.2 | Cell lines

Murine melanoma cell lines B16 and B16-BL6 were obtained from RIKEN Cell Bank (Tsukuba, Japan). Cells were cultured in DMEM supplemented with 10% FBS and penicillin-streptomycin (Nacalai Tesque, Kyoto, Japan).

2.3 | Antisense oligonucleotides

Antisense oligonucleotides (ASO) were prepared by Axolabs (Kulmbach, Germany). The nucleotide sequence of an ASO targeting mouse periostin mRNA is 5′-^{m}C*A*^{m}C*^{m}C*A*^{m}c*t*g*t*t* ^{m}c*g*t*a*a*U*U*U*G*G-3′ and that of a control oligonucleotide is 5′-^{m}C*G*A*^{m}C*A*t* ^{m}c*g*t*g*^{m}c*g*t* ^{m}c*g*U*A*U*A*U-3′, with lowercase letters indicating deoxyribonucleotides and underlined uppercase letters denoting 2′-O-methyl-ribonucleotides. The nucleobases indicated as ^{m}C and ^{m}c are 5-methylcytosine. Asterisks indicate that internucleotide linkages are phosphorothioate.

2.4 | In vivo studies

For establishment of a lung metastasis model, 50 μL (0.025 U) bleomycin (Cayman Chemical, Ann Arbor, MI, USA) or 50 μL saline were given to mice intratracheally. After 10 days, B16 cells (1×10^5) were injected into the tail vein, and the mice were killed 11 days later. For evaluation of the time course of lung fibrosis induced by bleomycin, mice were killed 4, 8, 12, and 16 days after receiving bleomycin. Non-treated mice were examined as the time 0 control. For analysis of the effect of giving ASO on fibrosis, mice were treated intratracheally with control or 100 μg periostin ASO 2 and 7 days after receiving bleomycin and were killed 8 days after receiving bleomycin. For analysis of the effect of ASO dosage on metastasis, mice were treated intratracheally with control or periostin ASO at 2 and 7 days, injected into the tail vein with B16 cells at 10 days, and killed at 21 days after receiving bleomycin.

2.5 | Tissue histology

Mice were killed by ip injection of pentobarbital (Kyoritsu Seiyaku, Tokyo, Japan), and perfused through the right cardiac ventricle with PBS. The lungs were inflated with 4% paraformaldehyde, dissected, incubated in 4% paraformaldehyde overnight, and embedded in paraffin. Tissue sections with a thickness of 2 μm were subjected to Masson's trichrome staining, and those with a thickness of 3 μm were stained with hematoxylin-eosin (H&E) or subjected to immunohistochemical or immunohistofluorescence analysis. Immunohistochemistry was carried out with antibodies to MelanA (mouse monoclonal, ab731; Abcam, Cambridge, UK), to periostin (mouse monoclonal, clone no. SS19C),[16] or to α-SMA (rabbit polyclonal, ab5694; Abcam), and immune complexes were detected with the use of a Vectastain Elite ABC-HRP Kit and Mouse on Mouse Immunodetection Kit (Vector, Burlingame, CA, USA). Immunohistofluorescence staining was carried out with antibodies to MelanA (as above), to periostin (rabbit polyclonal, ab14041; Abcam), or to Ki-67 (rabbit monoclonal, MA5-14520; Thermo Fisher Scientific, Waltham, MA, USA) or with eFluor 660-conjugated antibodies to α-SMA (mouse monoclonal, 50-9760-82; Thermo Fisher Scientific). Immune complexes were detected with Alexa Fluor 488-, Alexa Fluor 555-, or Alexa Fluor 594-conjugated goat antibodies to rabbit or mouse IgG (Thermo Fisher Scientific), and nuclei were stained with DAPI

(Sigma Chemical Co., St Louis, MO, USA). Tissue sections were viewed with a Biorevo BZ-9000 fluorescence microscope (Keyence, Osaka, Japan), a TissueFAXS Histo light microscope (TissueGnostics, Vienna, Austria), or an FV1000-D confocal microscope (Olympus, Tokyo, Japan). Tumor size (mm^2) and cell counts were quantitated with the use of BZ-X Analyzer and HistoQuest. Three random fields for each of at least 3 mice per group were assessed for tumor size, cell counts, and severity of fibrosis based on the Ashcroft score.[17]

2.6 | Statistical analysis

Data are presented as means ± SD and were analyzed with Student's *t* test or one-way ANOVA followed by Dunnett's multiple comparison test as carried out with GraphPad Prism version 6. *P*-value of <.05 was considered statistically significant.

2.7 | Additional methods

Isolation and culture of murine lung fibroblasts, in vivo studies for analysis of the effect of giving ASO on metastasis by B16-BL6, quantitative RT-PCR analysis, and periostin ASO treatment in vitro are described in Appendix S1.

3 | RESULTS

3.1 | Expression of periostin and number of α-SMA⁺ cells increase with progression of bleomycin-induced lung fibrosis

To examine the relation between fibrotic change and periostin expression in mouse lung, we studied a well-characterized mouse model of lung fibrosis based on bleomycin treatment.[18] C57BL/6J mice that received a single intratracheal injection of bleomycin were subjected to histological analysis of the lung every 4 days for up to 16 days (Figure 1A). An increase in interstitial thickness was apparent from day 4 and was followed by an increase in fibrosis, with marked accumulation of connective tissue and collapse of alveolar structure being observed from day 12. Ashcroft score for severity of fibrosis was significantly increased from day 8 to day 16 compared with that at day 0 (Figure 1B). Progression of lung fibrosis was accompanied by a pronounced increase in the number of periostin⁺ cells that was first apparent at day 8 (Figure 1A,C). Number of α-SMA⁺ myofibroblasts, which are key mediators of fibrosis,[19] was also increased in fibrotic lesions at day 8 but had decreased again at day 12 (Figure 1D,E).

3.2 | Bleomycin-induced lung fibrosis promotes metastatic colonization by melanoma cells in association with increased periostin expression

Lung metastatic colonization was previously shown to be increased in mice treated with bleomycin before injection of 4T1 murine breast tumor cells with a high lung metastatic potential, suggesting that a

fibrotic microenvironment may serve as a niche conducive to tumor cell colonization.[5] To investigate whether bleomycin treatment promotes lung colonization by tumor cells with a low metastatic potential, such as B16 murine melanoma cells, we injected B16 cells into the tail vein of mice 10 days after giving intratracheal bleomycin (Figure 2A). Number of macrometastases and tumor burden determined 11 days later were significantly increased in the bleomycin-treated mice compared with saline-treated control animals, in which metastasis was rarely observed (Figure 2B,C), indicating that a fibrotic environment promotes metastatic colonization and propagation of tumor cells with a low metastatic ability. Immunohistofluorescence analysis showed expression of periostin at metastatic sites (those positive for MelanA⁺ melanoma cells) in the lungs not only of bleomycin-treated mice but also in those of saline-treated controls (Figure 2D) in spite of the fact that expression of periostin was quite low in B16 cells (Figure S1), implying that periostin in metastatic colonization of the lung is produced by fibroblasts.

3.3 | Periostin ASO suppresses fibrosis and the increase in α-SMA⁺ cell number in lungs of bleomycin-treated mice

To clarify the role of periostin in lung fibrosis induced by bleomycin, we gave an ASO targeting periostin mRNA to inhibit periostin expression.[20] We confirmed that periostin ASO suppressed *Postn* mRNA expression in lung fibroblasts in vitro (Figure S2). Mice were thus injected intratracheally with a control or periostin ASO on day 2 and day 7 after receiving bleomycin, and the lung was subjected to histological analysis on day 8. We found that periostin ASO treatment attenuated lung fibrosis as well as periostin expression induced by bleomycin (Figure 3A). Both the Ashcroft score and the percentage of periostin⁺ cells were thus significantly lower in the mice treated with periostin ASO than in those that received control ASO (Figure 3B,C). The number of α-SMA⁺ cells in fibrotic lesions was also reduced by periostin ASO treatment (Figure 3D). Of note, cells positive for both Ki-67 and α-SMA, corresponding to proliferating myofibroblasts, were observed less frequently in fibrotic loci of periostin ASO-treated mice (Figure 3E). These data suggested that periostin plays a key role in the development of lung fibrosis and myofibroblast activation in response to bleomycin.

3.4 | Periostin ASO suppresses lung metastasis of B16 murine melanoma cells promoted by lung fibrosis

Given that periostin ASO attenuated lung fibrosis induced by bleomycin, we examined whether knockdown of periostin expression might also inhibit metastatic colonization of the lung promoted by pulmonary fibrosis. Mice were treated intratracheally with control or periostin ASO at 2 and 7 days after receiving bleomycin and were injected i.v. with B16 cells at 10 days (Figure 4A). Number of macrometastases (Figure 4B) as well as tumor burden (Figure 4C) in the lung at day 21 was significantly reduced in the periostin ASO-treated mice compared with the control animals. These results thus
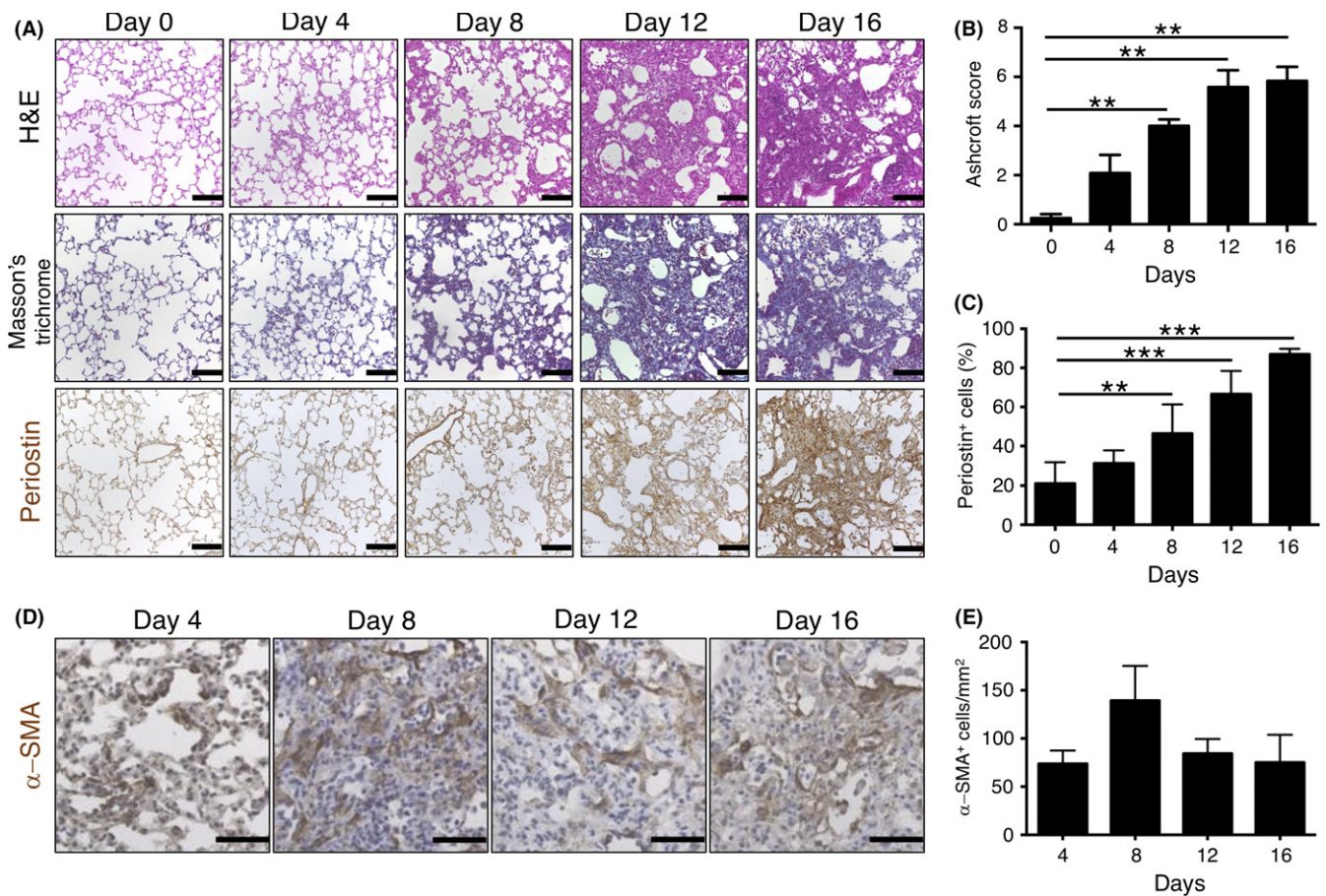
FIGURE 1 Up-regulation of periostin expression associated with progression of lung fibrosis. A, Serial sections of the lung from non-treated mice (Day 0) and mice killed 4, 8, 12, or 16 d after receiving intratracheal bleomycin were subjected to hematoxylin-eosin (H&E) and Masson's trichrome staining as well as to immunohistochemical analysis with antibodies to periostin. Scale bars, 100 μm. B, Ashcroft score for lung fibrosis and C, percentage of periostin-positive cells in the lungs of mice treated as in (A). D, Sections of the lung from mice treated as in A, were subjected to immunohistochemical analysis of α-smooth muscle actin (α-SMA) expression. Scale bars, 50 μm. E, Density of α-SMA-positive cells in fibrotic areas of the lung from mice treated as in (A). All quantitative data are means ± SD for 4 mice in each group. **$P < .01$, ***$P < .001$ (one-way ANOVA)

indicated that inhibition of periostin expression suppressed metastatic colonization of the lung by tumor cells by preventing formation of a fibrotic milieu that can serve as a premetastatic niche.

4 | DISCUSSION

We have herein confirmed that periostin is widely expressed in fibrotic lesions of C57BL/6J mice with bleomycin-induced lung fibrosis. Periostin expression has previously been shown to be up-regulated in lung mesenchymal cells such as fibroblasts and fibrocytes in mice treated with bleomycin,[21] in monocytes, fibrocytes, and fibroblasts of the lung in patients with idiopathic pulmonary fibrosis,[15] and in bronchial epithelial cells of such patients and individuals with asthma.[22] Bleomycin treatment has also been found to increase the expression of various inflammatory mediators including transforming growth factor-β1 (TGF-β1), interleukin (IL)-4, and IL-13.[23] Up-regulation of periostin production in lung cells might thus be mediated through activation of TGF-β or JAK-STAT signaling pathways.[21,24]

Myofibroblasts play the leading role in tissue remodeling and production of ECM during lung fibrogenesis. Consistent with this scenario, we found that the number of α-SMA+ myofibroblasts increased concomitantly with that of periostin+ cells in the lung of bleomycin-treated mice. Myofibroblasts that originate from resident stromal cells are activated by various stimuli including chemokines, ECM proteins, and mechanical stress.[25] Periostin up-regulates α-SMA expression in murine skin fibroblasts through activation of integrin-FAK signaling.[26] Periostin also promotes the induction of myofibroblast differentiation by cytokines such as TGF-β1 and connective tissue growth factor, the latter of which is secreted from lung mesenchymal cells in response to bleomycin stimulation.[21] Periostin may therefore play an important role in bleomycin-induced lung fibrosis through activation of myofibroblasts and consequent ECM accumulation.

Metastatic colonization is thought to be problematic for tumor cells because most of the cells die of maladaptation to the new microenvironment which rejects tumor cells by multiple factors including reactive oxygen species (ROS), hypoxia, inhibitory
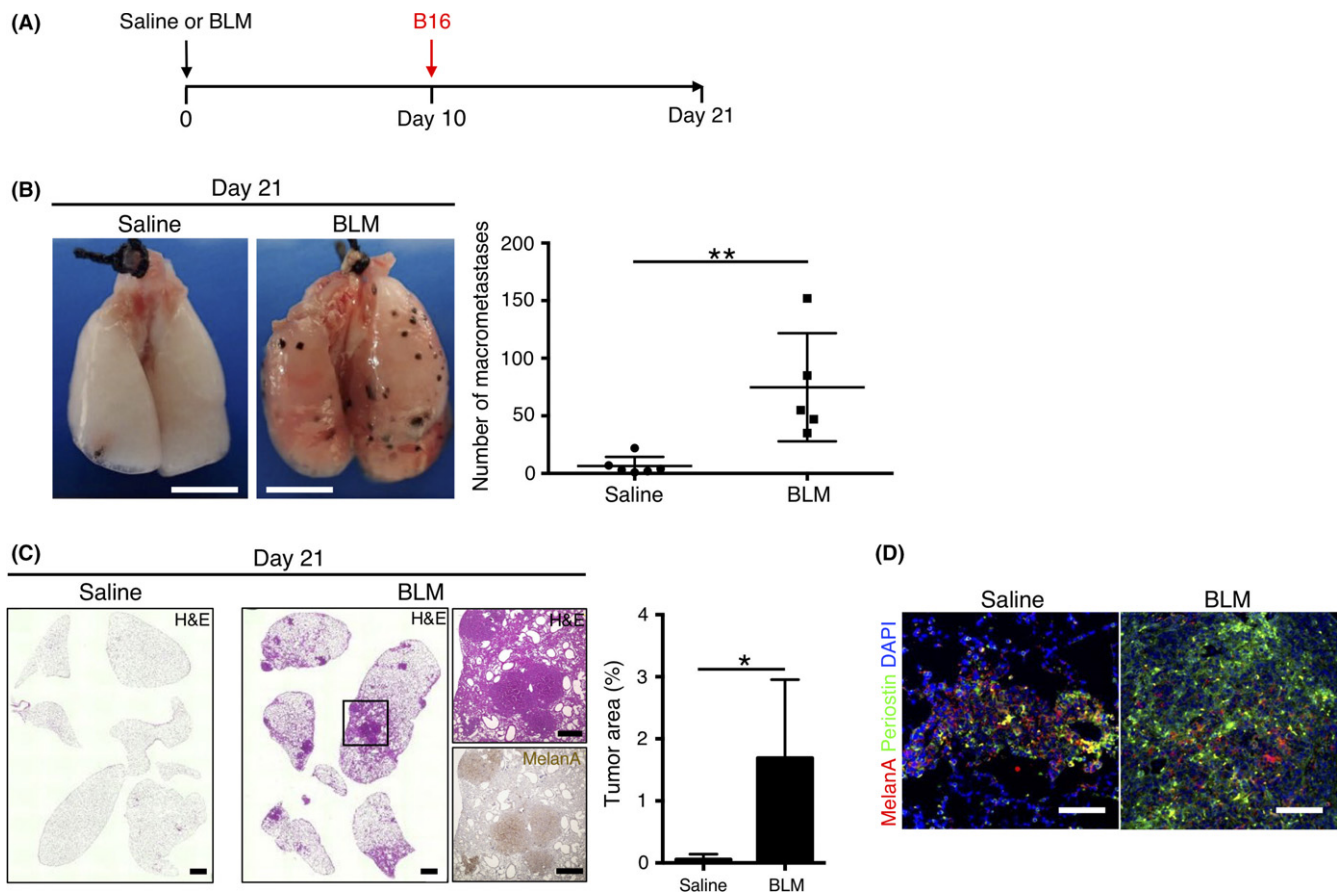
FIGURE 2 Bleomycin-induced lung fibrosis promotes lung metastasis of B16 melanoma cells. A, Schematic representation of the experimental protocol. Mice received bleomycin (BLM) or saline intratracheally (i.t.) 10 d before injection of B16 murine melanoma cells into the tail vein. Mice were killed for analysis 11 d after cell injection. B, Representative images of the lungs of mice at day 21 and quantification of the number of macroscopically detectable lung metastases. Scale bars, 5 mm. Quantitative data are for individual mice and means $\pm$ SD for each group. C, Hematoxylin-eosin (H&E) staining and immunohistochemical analysis of MelanA as well as quantification of the percentage tumor area based on MelanA staining for the lungs of mice killed on day 21. The boxed area in the low-magnification image of bleomycin-treated lung tissue is shown at higher magnification in the images on the right. Scale bars represent 1 mm and 100 μm for low- and high-magnification images, respectively. Quantitative data are means $\pm$ SD for 5 (bleomycin) or 6 (saline) mice. D, Representative immunohistofluorescence staining of MelanA and periostin in metastatic tumors from saline- or bleomycin-treated mice on day 21. Nuclei were stained with DAPI. Scale bars, 100 μm. *P < .05, **P < .01 (Student's t test)

cytokines and immune cells,[27] and only a few of those that survive go on to give rise to macrometastases.[28] ROS is known to be a major contributor to prevention of tumor cell metastasis. It is known that some kinds of ECM proteins such as laminin and fibronectin stimulate the generation of ROS by integrin-mediated signaling pathway.[29] In contrast, fibulin-5 reduced ROS production in pancreatic cancer cells by competing with fibronectin for binding to integrin.[30] Therefore, an ECM protein periostin might also be involved in the regulation of ROS level in the premetastatic niche. An experimental mouse model showed that only 0.02% of melanoma cells injected into the portal vein were able to form multicellular foci in the liver.[31] Similarly, we found that macrometastases in saline-treated mouse lung were rarely observed after tail vein injection of B16 melanoma cells. In contrast, a large number of macrometastases was evident in the bleomycin-treated lung, suggesting that the generation of a fibrotic milieu in the lung by giving bleomycin promoted metastatic colonization by melanoma cells. To assess the role of

periostin in the development of lung fibrosis and consequent promotion of tumor cell colonization, we gave an ASO targeting periostin mRNA intratracheally in order to inhibit periostin expression in the lung. ASO were first developed in the form of a short DNA fragment tested in vitro in 1978,[32] and they have recently proven therapeutically effective in several clinical trials for conditions such as hypercholesterolemia[33] and malignant tumors.[34,35] Current gapmer ASO, including those used in the present study, contain both a central deoxynucleotide phosphorothioate gap that allows them to promote cleavage of target mRNA by recruiting ribonuclease H to the ASO/target mRNA heteroduplex site as well as 5′- and 3′- wing regions modified with 2′-O-methoxyethyl or 2′-O-methyl residues that increase both resistance to degradation and affinity for the target mRNA.[36] Although the delivery of ASO to the desired organs and cells remains to be optimized, these molecules have the potential to be developed into unprecedented therapies given their high target specificity.[37]
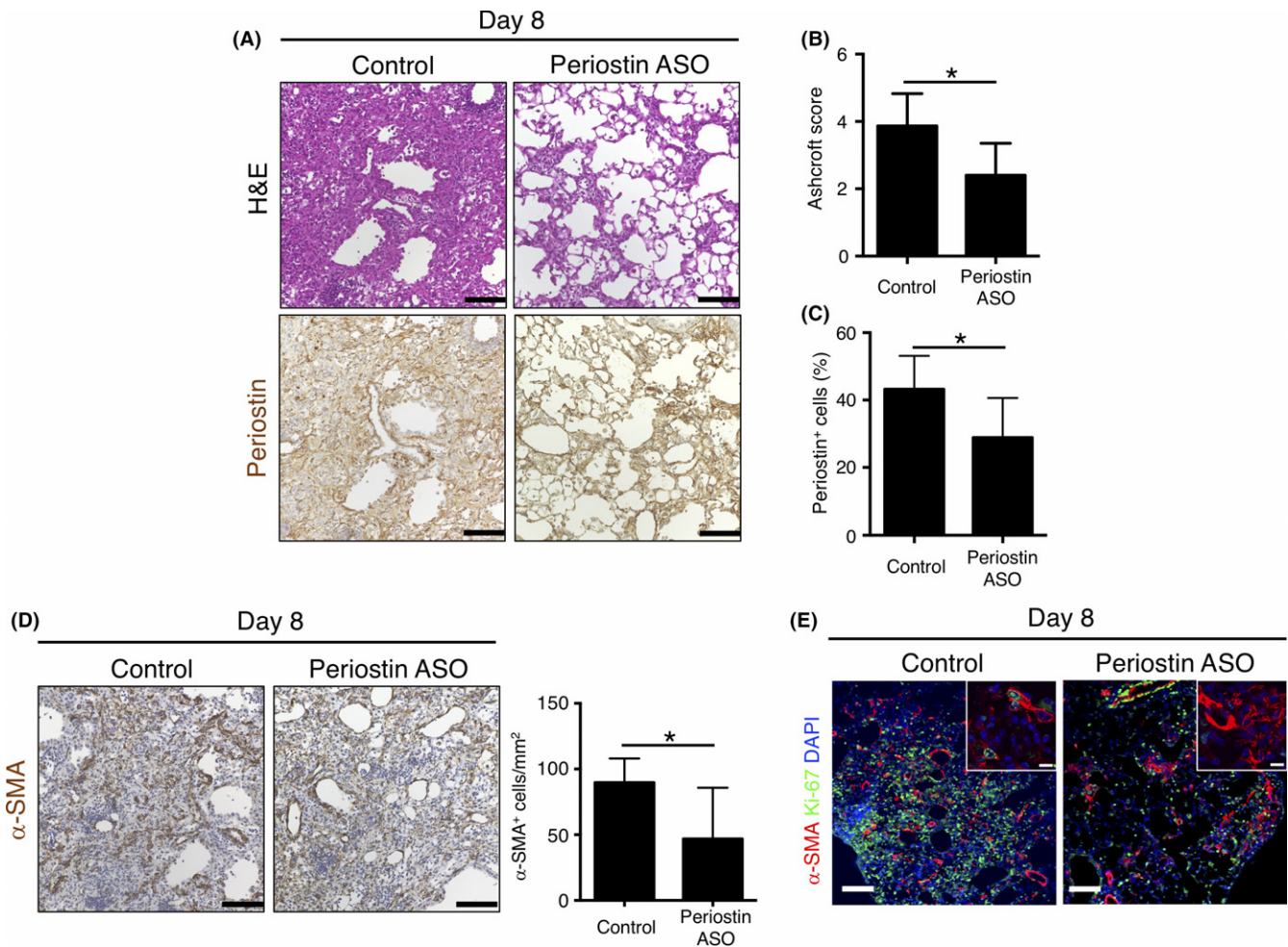
FIGURE 3 Effects of giving periostin antisense oligonucleotides (ASO) on the bleomycin-treated lung. A, Mice were injected intratracheally with a control or periostin ASO at 2 and 7 d after receiving bleomycin and were killed for analysis on day 8. Serial sections of the lung were stained with hematoxylin-eosin (H&E) and subjected to immunohistochemical analysis of periostin expression. Scale bars, 100 μm. B, Ashcroft score for lung fibrosis in the mice on day 8. C, Quantification of the percentage of periostin-positive cells in the lung on day 8. D, Lung sections from the mice on day 8 were subjected to immunohistochemical analysis for quantification of the density of α-smooth muscle actin (α-SMA)-positive cells in fibrotic areas. Scale bars, 100 μm. E, Representative immunohistofluorescence staining of lung fibrotic lesions for α-SMA and Ki-67 at day 8. Nuclei were stained with DAPI. Scale bars, 100 and 10 μm for low-magnification and high-magnification (insets) images, respectively. All quantitative data are means ± SD for 8 and 6 mice injected with the control or periostin ASO, respectively. *$P < .05$ (Student's t test)

In the present study, we directed periostin ASO to lung cells by intratracheal administration. Such periostin ASO administration attenuated fibrosis and reduced the number of active myofibroblasts in the lung of bleomycin-stimulated mice. Furthermore, we found that the periostin ASO significantly inhibited metastatic colonization of the bleomycin-treated lung by melanoma cells. In addition, we carried out similar experiments using mice without BLM pretreatment and B16-BL6 cells which have a high metastatic potential (Figure S3A). Although the impact was somewhat limited, we observed that the number of lung macrometastases by B16-BL6 cells was decreased by periostin ASO treatment (Figure S3B). Collectively, our data thus indicate that inhibition of periostin expression ameliorated bleomycin-induced lung fibrosis through suppression of myofibroblast differentiation, resulting in

attenuation of ECM production. These results therefore suggest that periostin is one of the most important molecular contributors for formation of a fibrotic milieu that supports lung colonization by melanoma cells. In addition, we do not exclude other roles of periostin, such as adhesion to melanoma cells and maintenance of metastatic melanoma cells. At least, as an adhesion molecule, periostin is likely to associate with integrin of melanoma cells because periostin was actually expressed around metastatic melanoma regions in the lung (Figure 2D). Therefore, our data further suggest the possibility that periostin has a function that directly promotes metastatic colonization by melanoma cells even in non-fibrotic lungs.

In summary, our results provide evidence that periostin is an essential molecule for generation of bleomycin-induced lung fibrosis.
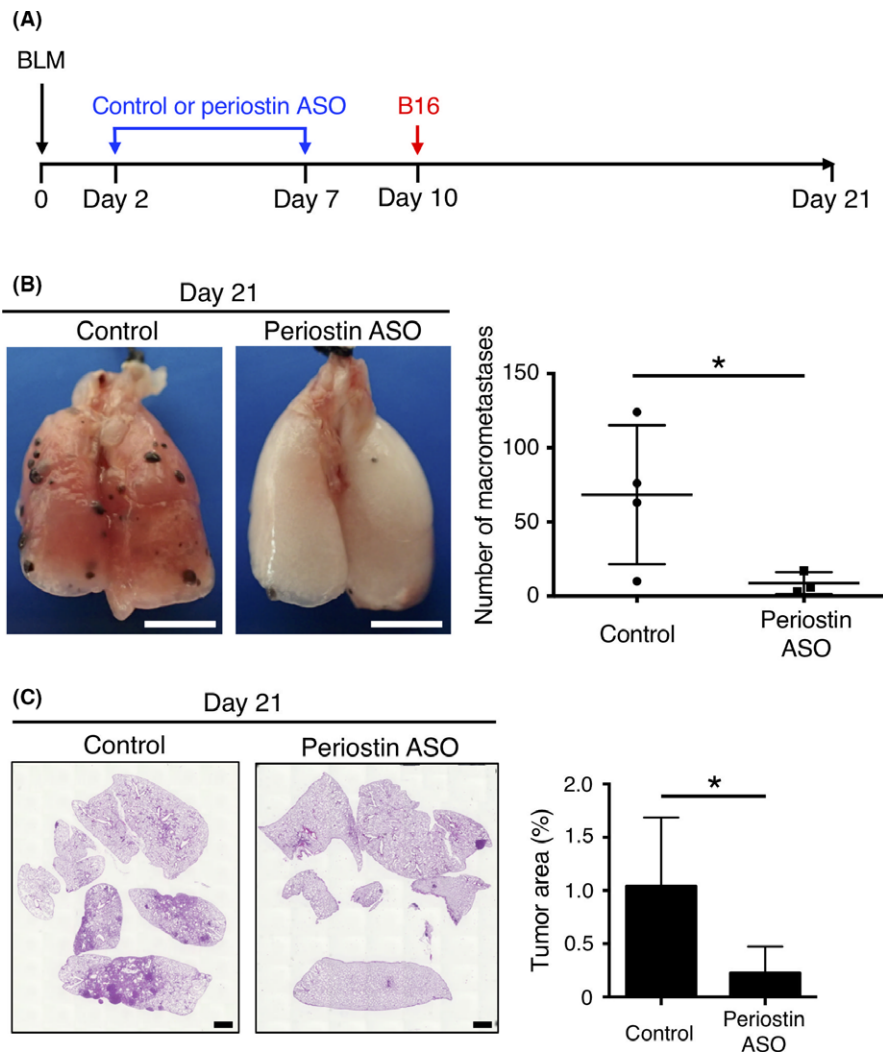
FIGURE 4 Inhibition of periostin expression suppresses metastasis of melanoma cells to the fibrotic lung. A, Schematic representation of the experimental protocol. Mice received bleomycin (BLM) intratracheally 10 d before tail vein injection of B16 murine melanoma cells. The mice were also injected intratracheally with control or periostin antisense oligonucleotides (ASO) 2 and 7 d after receiving bleomycin and were killed for analysis on day 21. B, Representative images of the lungs and quantification of the number of macroscopically detectable lung metastases at day 21. Scale bars, 5 mm. Quantitative data are for individual mice and means $\pm$ SD for each group. C, Hematoxylin-eosin (H&E) staining of lung tissue and quantification of the percentage tumor area based on immunohistochemical staining for MelanA at day 21. Scale bars, 1 mm. Data are means $\pm$ SD for 4 (control ASO) or 3 (periostin ASO) mice. *$P < .05$ (Student's t test)

Our results suggest that periostin promotes metastatic colonization of the lung by melanoma cells. Furthermore, ASO-based therapies that target periostin have the potential to suppress metastatic colonization by preventing the formation of a fibrotic milieu able to serve as a premetastatic niche.

CONFLICT OF INTEREST

M.Y., K.T., and K.Y. are employed by AQUA Therapeutics Co., Ltd. H.S. has received research grants from AQUA Therapeutics Co., Ltd. The remaining authors declare no financial conflicts of interest.

ORCID

Eiji Sugihara [iD] http://orcid.org/0000-0002-3233-1045

REFERENCES

1. Steeg PS. Targeting metastasis. *Nat Rev Cancer*. 2016;16:201-218.

2. Budczies J, von Winterfeld M, Klauschen F, et al. The landscape of metastatic progression patterns across major human cancers. *Oncotarget*. 2015;6:570-583.

3. Liu Y, Cao X. Characteristics and Significance of the Pre-metastatic Niche. *Cancer Cell*. 2016;30:668-681.

4. Bonnans C, Chou J, Werb Z. Remodelling the extracellular matrix in development and disease. *Nat Rev Mol Cell Biol*. 2014;15:786-801.

5. Cox TR, Bird D, Baker AM, et al. LOX-mediated collagen crosslinking is responsible for fibrosis-enhanced metastasis. *Cancer Res*. 2013;73:1721-1732.

6. Nielsen SR, Quaranta V, Linford A, et al. Macrophage-secreted granulin supports pancreatic cancer metastasis by inducing liver fibrosis. *Nat Cell Biol*. 2016;18:549-560.

7. Murin S, Inciardi J. Cigarette smoking and the risk of pulmonary metastasis from breast cancer. *Chest*. 2001;119:1635-1640.

8. Conway SJ, Izuhara K, Kudo Y, et al. The role of periostin in tissue remodeling across health and disease. *Cell Mol Life Sci*. 2014;71:1279-1288.

9. Tilman G, Mattiussi M, Brasseur F, van Baren N, Decottignies A. Human periostin gene expression in normal tissues, tumors and melanoma: evidences for periostin production by both stromal and melanoma cells. *Mol Cancer*. 2007;6:80.

10. Malanchi I, Santamaria-Martinez A, Susanto E, et al. Interactions between cancer stem cells and their niche govern metastatic colonization. *Nature*. 2011;481:85-89.

11. Fukuda K, Sugihara E, Ohta S, et al. Periostin is a key niche component for wound metastasis of melanoma. *PLoS One*. 2015;10: e0129704.

12. George EL, Georges-Labouesse EN, Patel-King RS, Rayburn H, Hynes RO. Defects in mesoderm, neural tube and vascular development in mouse embryos lacking fibronectin. *Development*. 1993;119:1079-1091.

13. Breindl M, Harbers K, Jaenisch R. Retrovirus-induced lethal mutation in collagen I gene of mice is associated with an altered chromatin structure. *Cell*. 1984;38:9-16.

14. Uchida M, Shiraishi H, Ohta S, et al. Periostin, a matricellular protein, plays a role in the induction of chemokines in pulmonary fibrosis. *Am J Respir Cell Mol Biol*. 2012;46:677-686.

15. Naik PK, Bozyk PD, Bentley JK, et al. Periostin promotes fibrosis and predicts progression in patients with idiopathic pulmonary fibrosis. *Am J Physiol Lung Cell Mol Physiol*. 2012;303:L1046-L1056.

16. Yamaguchi Y, Ono J, Masuoka M, et al. Serum periostin levels are correlated with progressive skin sclerosis in patients with systemic sclerosis. *Br J Dermatol*. 2013;168:717-725.

17. Ashcroft T, Simpson JM, Timbrell V. Simple method of estimating severity of pulmonary fibrosis on a numerical scale. *J Clin Pathol*. 1998;41:467-470.

18. Moore BB, Hogaboam CM. Murine models of pulmonary fibrosis. *Am J Physiol Lung Cell Mol Physiol*. 2008;294:L152-L160.

19. Wynn TA, Ramalingam TR. Mechanisms of fibrosis: therapeutic translation for fibrotic disease. *Nat Med*. 2012;18:1028-1040.

20. Tomaru A, Kobayashi T, Hinneh JA, et al. Oligonucleotide-targeting periostin ameliorates pulmonary fibrosis. *Gene Ther*. 2017;24:706-716.

21. Ashley SL, Wilke CA, Kim KK, Moore BB. Periostin regulates fibrocyte function to promote myofibroblast differentiation and lung fibrosis. *Mucosal Immunol*. 2017;10:341-351.

22. Sidhu SS, Yuan S, Innes AL, et al. Roles of epithelial cell-derived periostin in TGF-beta activation, collagen production, and collagen gel elasticity in asthma. *Proc Natl Acad Sci USA*. 2010;107:14170-14175.

23. Belperio JA, Dy M, Burdick MD, et al. Interaction of IL-13 and C10 in the pathogenesis of bleomycin-induced pulmonary fibrosis. *Am J Respir Cell Mol Biol*. 2002;27:419-427.

24. Chandriani S, DePianto DJ, N'Diaye EN, et al. Endogenously expressed IL-13Ralpha2 attenuates IL-13-mediated responses but does not activate signaling in human lung fibroblasts. *J Immunol*. 2014;193:111-119.

25. Hinz B, Phan SH, Thannickal VJ, Galli A, Bochaton-Piallat ML, Gabbiani G. The myofibroblast: one function, multiple origins. *Am J Pathol*. 2007;170:1807-1816.

26. Elliott CG, Wang J, Guo X, et al. Periostin modulates myofibroblast differentiation during full-thickness cutaneous wound repair. *J Cell Sci*. 2012;125:121-132.

27. Gupta GP, Massague J. Cancer metastasis: building a framework. *Cell*. 2006;127:679-695.

28. Massague J, Obenauf AC. Metastatic colonization by circulating tumour cells. *Nature*. 2016;529:298-306.

29. Edderkaoui M, Hong P, Vaquero EC, et al. Extracellular matrix stimulates reactive oxygen species production and increases pancreatic cancer cell survival through 5-lipoxygenase and NADPH oxidase. *Am J Physiol Gastrointest Liver Physiol*. 2005;289:G1137-G1147.

30. Wang M, Topalovski M, Toombs JE, et al. Fibulin-5 Blocks Microenvironmental ROS in Pancreatic Cancer. *Cancer Res*. 2015;75:5058-5069.

31. Luzzi KJ, MacDonald IC, Schmidt EE, et al. Multistep Nature of Metastatic Inefficiency: dormancy of solitary cells after successful extravasation and limited survival of early micrometastases. *Am J Pathol*. 1998;153:865-873.

32. Zamecnik PC, Stephenson ML. Inhibition of Rous sarcoma virus replication and cell transformation by a specific oligodeoxynucleotide. *Proc Natl Acad Sci USA*. 1978;75:280-284.

33. Raal FJ, Santos RD, Blom DJ, et al. Mipomersen, an apolipoprotein B synthesis inhibitor, for lowering of LDL cholesterol concentrations in patients with homozygous familial hypercholesterolaemia: a randomised, double-blind, placebo-controlled trial. *Lancet*. 2010;375:998-1006.

34. Chia S, Dent S, Ellard S, et al. Phase II trial of OGX-011 in combination with docetaxel in metastatic breast cancer. *Clin Cancer Res*. 2009;15:708-713.

35. Beer TM, Hotte SJ, Saad F, et al. Custirsen (OGX-011) combined with cabazitaxel and prednisone versus cabazitaxel and prednisone alone in patients with metastatic castration-resistant prostate cancer previously treated with docetaxel (AFFINITY): a randomised, open-label, international, phase 3 trial. *Lancet Oncol*. 2017;18:1532-1542.

36. Kole R, Krainer AR, Altman S. RNA therapeutics: beyond RNA interference and antisense oligonucleotides. *Nat Rev Drug Discov*. 2012;11:125-140.

37. Frazier KS. Antisense oligonucleotide therapies: the promise and the challenges from a toxicologic pathologist's perspective. *Toxicol Pathol*. 2015;43:78-89.

SUPPORTING INFORMATION

Additional Supporting Information may be found online in the supporting information tab for this article.